Analysis of fiber gratings by external Bragg reflection.

Reinhard Ulrich

Technische Universität Hamburg-Harburg
21071 Hamburg, Germany

8.September 1995

submitted to: IEEE Journal of Lightwave Technolgy)

Indexing terms: *gratings, fiber gratings, Bragg reflection*

Abstract

A dielectric grating in the core of a single-mode fiber, designed for internal Bragg reflection of wavelength λ_B, may be analyzed by Bragg reflecting an external laser beam of a shorter wavelength ($\lambda < \lambda_B/n_o$), focused through the wall of the fiber onto its core (index n_o). By scanning the probe beam along the fiber and measuring the reflected power and the angular deflection, the envelope of the index modulation $\Delta n(z)$ and the chirp function $g(z)$ of the fiber grating can be determined. This method is analyzed theoretically with respect to the resolutions attainable in z, Δn, and g for simple, non-slanted fiber gratings.

I. Introduction:

Fiber gratings written by UV exposure into the Ge doped core of silica optical fiber [1] are rapidly finding applications in optical communications [2] and sensor technology. [3] Chirped gratings, in which the grating period g and/or the amplitude Δn of the index modulation vary along the axial direction z of the fiber, are promising as broad-band filters and delay equalizers. [4] Especially for such advanced gratings, methods are required to measure with good accuracy the axial envelope functions $g(z)$ and $\Delta n(z)$ of the grating during or after fabrication, because highly sophisticated envelopes are envisaged. Recently it has been shown that these profiles may be determined by an inverse scattering procedure from reflectometric data, measured at both ends of the grating with light guided by the fiber core. [5] This method has the advantage that the grating is analyzed at the very wavelengths at which it is designed to operate. Nevertheless, this method is indirect and relies for evaluation on a sophisticated algorithm, and for long gratings the results may be corrupted in intricate ways by measuring errors.

A fairly direct method [6] free of these problems employs the Bragg reflection of a short-wavelength external probe beam of light which falls through the side of the fiber on its core, see Fig. 1(a). When its free-space wavelength λ is short enough and the angle θ_i of incidence is adjusted to satisfy an external Bragg condition, a fraction P_B of the input power P_i is reflected by the fiber grating into a narrow output beam in the direction $\psi_i \approx \theta_i$. The power of this Bragg reflected beam is proportional to Δn^2 if the grating in the fiber core can be described by an axial index distribution of the form $n(z) = \overline{n_o} + \Delta n \cos(2\pi z/g)$. Therefore, when the amplitude Δn of the index modulation varies gradually along the fiber, $\Delta n = \Delta n(z)$, this envelope function can be determined directly from a measurement of $P_B(z)$. By measuring the angle $(\psi_i + \theta_i)$ of deflection of the output beam relative to the input beam, it should also be possible to determine the chirp function $g(z)$ of the grating.

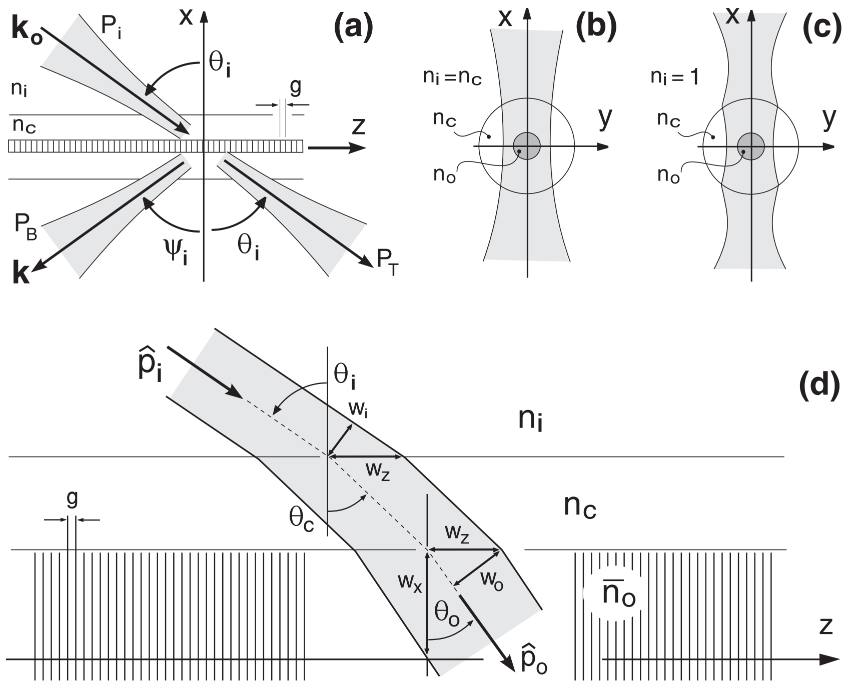

Figure 1: Geometry of Bragg reflection of an external probe beam by a fiber grating. (a) general input and output directions of a fiber with a grating in the core region; side view; (b) axial view in a situation of immersion ($n_i = n_c$); (c) axial view in a free-space arrangement; (d) transformations of the beam cross-section and of the waist radii.

Applying elementary optical principles [7], the situation of this measurement may be described by the conditions for the 1st order diffraction by grating of period g, and accounting for the refraction of the input beam (angles θ_μ) and output beam (angles ψ_μ) at the interfaces between the various media of index n_μ. We abbreviate $\mu =$i: input medium, c: cladding, and o: core of the fiber.

$$n_i\ (\sin\theta_i\ +\ \sin\psi_i\ )\ =\ \lambda/g \tag{1}$$
$$n_i\ \sin\theta_i\ =\ n_c\ \sin\theta_c\ =\ \overline{n_o}\ \sin\theta_o \tag{2}$$
$$n_i\ \sin\psi_i\ =\ n_c\ \sin\psi_c\ =\ \overline{n_o}\ \sin\psi_o \tag{3}$$

In these relations λ is the free-space wavelength, and the *average* index of the region of the fiber grating is denoted by $\overline{n_o}$. We postulate that the index planes of the grating, resulting from the UV exposure, are normal to the axis of the fiber. This 'non-slanted' arrangement is optimum for the Bragg retro-reflection, as it couples least to the cladding modes in that usage. While these equations fix the direction of a diffracted beam, appreciable power can be expected in that direction only if in addition to Eqs.(1)-(3) the classical Bragg condition is satisfied for the fiber grating. [7]

$$n_o\ \sin\theta_o\ =\ n_o\ \sin\psi_o\ =\ \lambda/2g. \tag{4}$$

Consequently, the directions of input and output are symmetric to the fiber axis, and $\theta_\mu = \psi_\mu$ for $\mu =$o, c, and i. This is the arrangement used in the application [6] of such an external Bragg reflection for the determination of the index modulation $\Delta n(z)$. It may be characterized by stating that the fiber grating behaves like a 'thin' grating, obeying Eq.(1), which is 'blazed' for the symmetric (Bragg) situation.

In the following, the validity of this description will be shown. In particular, the diffraction efficiency will be analyzed qualitatively and quantitatively for a Gaussian input beam. As the index modulation is typically weak ($\Delta n \leq 10^{-3}$), the calculation is performed in the limit of weak scattering. This approximation leads to the following organization of the paper. In Sec. II the illuminated part of the grating is treated as a perturbation of the probe beam, producing a three-dimensional distribution of electric dipole moments. They emit the diffracted output beam. Its angular power distribution and the total diffracted power are derived in Sec. III as functions of the geometry and polarization of the input beam and of the grating parameters. These relations are required for the evaluation of $\Delta n(z)$ and $g(z)$ from the measurements. The results are discussed in Sec. IV with respect to the role of experimental tolerances, the attainable spatial resolution Δz and the possibility of measuring small index modulations Δn. Finally, a proposal is made for the precise determination of g(z).

II. Excitation of the fiber grating

Calculating the diffracted beam means to find a solution of the wave equation for the given index distribution of fiber and grating and for the given incident probe beam. An approximate solution is derived here by treating the grating as a perturbation of a situation in which the probe beam propagates freely through the fiber at the Bragg angle θ_o. The beam position z_o is initially assumed to be fixed, $z_o = 0$, and the argument z_o will be suppressed throughout. The diffraction efficiency which results from this calculation may then be used to evaluate $\Delta n(z)$ from a scan of the beam position z_o along the fiber, provided the variation of $\Delta n(z)$ is sufficiently slow.

In the absence of a grating, the probe beam passes through the fiber and may become slightly deformed because the fiber and the core act as a cylindrical lens. This 'unperturbed' situation is characterized by an electric field distribution $\mathbf{E}_o(\mathbf{r})$. The grating is introduced now as an additive modification $\delta\epsilon(\mathbf{r})$ of the dielectric permittivity $\epsilon = n^2(\mathbf{r})\,\epsilon_o$. Compared to the situation without grating, in each volume element $dV = dx\,dy\,dz$ an electric dipole moment $d\mathbf{q}$ results.

$$d\mathbf{q} \;=\; \delta\epsilon(\mathbf{r})\;\mathbf{E}_o(\mathbf{r})\,dV \;=\; 2\,n_o\,\epsilon_o\,\delta n(\mathbf{r})\,\mathbf{E}_o(\mathbf{r})\,dV \qquad (5)$$

The points in the core region are described by the vector $\mathbf{r} = \{x, y, z\}$ in a Cartesian coordinate system, aligned to the fiber and the direction of the input beam, see Fig. 1. The index distribution $\delta n(\mathbf{r})$ of the fiber grating is separated into a transverse part $h(x, y)$ which is normalized to $Max(h) = 1$, and a grating part which depends periodically on z. From the latter part, only the fundamental space harmonic is considered here which is dominant. It is characterized by the periodicity $K = 2\pi/g$ and by the slowly varying amplitude $\Delta n(z)$ of the index variation.

$$\delta n(\mathbf{r}) \;=\; h(x, y)\,\Delta n(z)\;\cos(Kz) \qquad (6)$$

This separation of $\delta n(\mathbf{r})$ is legitimate if the grating is written by a single-photon process, because in that case the index variations can be expected to be similar across all transverse planes of the grating. [8]

Each dipole moment $d\mathbf{q}$ oscillates at the frequency ω of the probe beam and emits a scattered wave. Such radiating dipoles exist throughout that volume of the grating which is illuminated by the probe beam. The output beam results as the superposition of the fields emitted by all those dipoles.

This calculation, which represents a solution of the wave equation by a Green's function, is justified here in a situation of weak dielectric perturbation and small diffraction efficiency. In a typical single-mode fiber, both the incident and the scattered wave propagate essentially unaffected by the presence of the dielectric core and of the fiber grating. A wave which passes through the core or which originates inside the core experiences only a small extra phase delay, $\delta\phi \lesssim 2\,ka\,(n_o - n_c)$, as compared to a wave which propagates through a homogeneous medium of cladding index n_c. Here n_o is the index of the fiber core, and a is the core radius. For a typical fiber $\delta\phi \leq 0.2$.

It is postulated now that the probe beam is a Gaussian beam, and that its waist is focused on the fiber axis. It is further required that the waist radius w_o in the core region is considerably wider than the core, yet small compared to the outer fiber diameter. In this situation the field $\mathbf{E}_o(\mathbf{r})$ of the probe beam may be treated as a plane wave. Experimentally this focusing condition can be satisfied by the use of an immersion arrangement, in which the index n_i of the input medium is equal to the cladding index, $n_i = n_c$, see Fig. 1(b). Focusing may be achieved here with a simple lens, used on-axis. Alternatively, the probe beam may be incident from free space, $n_i = 1$. In this case the necessary waist on the fiber axis can be obtained only if an auxiliary waist is produced first in the xy view of Fig. 1(c) a short distance in front of the fiber, without affecting the beam profile in the xz view of Fig. 1(a). The outer fiber surface, acting as a cylindrical lens, projects the auxiliary waist into the waist on the fiber axis. A third waist forms in the transmitted beam behind the fiber. To realize this geometry the incident, originally circularly symmetric or 'stigmatic' [7] probe beam may be focused by an astigmatic optical system, providing a longer focal length for rays in the xz plane than for rays in the orthogonal plane. Such an astigmatism can be introduced conveniently by focusing with a spherical lens which is tilted from axial alignment about an axis in the xz plane, normal to the beam.

For simplicity we perform the analysis for a situation where the direction of incidence of the probe beam has been adjusted to satisfy a Bragg condition. This means

$$\lambda/2g \;=\; \overline{n_o}\,\sin\theta_o \;=\; n_c \sin\theta_c \;=\; n_i \sin\theta_i \;. \tag{7}$$

Deviations from this conditions will be considered later. Here it is important to note from Eq.(7) that the optimum external Bragg angle θ_i, which is directly accessible to measurement, is independent of the indices $\overline{n_o}$ and n_c and, therefore, of the entire radial index profile of the fiber. In particular, the external Bragg angle θ_i is not modified by axial variations of the mean index $\overline{n_o}$ of the core which typically result from the UV exposure. [8] In the following calculation of the diffraction efficiency, therefore, the small difference between core index n_o (before exposure) and $\overline{n_o}$ (after exposure) will be ignored. According to all assumptions made, the field of the probe beam is expressed as

$$\mathbf{E}_o(\mathbf{r}) \;=\; \hat{\mathbf{E}}_o\, G(\mathbf{r})\, e^{-j\mathbf{k}_o\mathbf{r}} \tag{8}$$

where
$$G(\mathbf{r}) \;=\; \exp\left[-\left(\frac{x}{w_x}\right)^2 - \left(\frac{y}{w_y}\right)^2 - \left(\frac{z}{w_z}\right)^2\right] \tag{9}$$

and
$$\mathbf{k}_o \;=\; n_o\, k\,\{-\cos\theta_o,\; 0,\; \sin\theta_o\} \tag{10}$$

Here, $k = |\mathbf{k}_o| = \omega/c = 2\pi/\lambda$ is the free-space wavenumber, and the time dependence $\exp(j\omega t)$ has been suppressed. The vector $\mathbf{k}_o$ characterizes the mean direction of propagation of the probe beam in the core region. The beam profile there results by refraction at the two interfaces $n_i/n_c/n_o$ from the Gaussian input beam. The latter converges to a (virtual) focal spot of waist radius w_i in the input medium n_i. According to the focusing conditions mentioned, the profile of the probe beam in the core region is Gaussian, too, with a waist of radius w_o at the origin. This profile is described in normalized form by the function $G(\mathbf{r})$ in Eq.(8). The waist radii w_x, w_y, and w_z are measured along the x, y, z coordinate axes, respectively. They are related to w_o and w_i by simple geometric relations which follow from Fig. 1(d).

$$w_o \;=\; w_x \sin\theta_o \;=\; w_y \;=\; w_z \cos\theta_o \;=\; w_i \cos\theta_o / \cos\theta_i \tag{11}$$

The peak optical power densities in these waists are $\hat{p}_i$ and $\hat{p}_o$, referring to the input medium and to the core region, respectively. In the given approximation, these power densities are related to the electrical field strength $\hat{\mathbf{E}}_o$ and to the total power P_o of the probe beam in the core region.

$$P_o \;=\; \frac{\pi}{2} w_i^2 \,\hat{p}_i \;=\; \frac{\pi}{2} w_o^2 \,\hat{p}_o \;=\; \frac{\pi}{4} n_o \, Y_o \, w_o^2 \, \hat{\mathbf{E}}_o^2 \tag{12}$$

Here $Y_o = (\epsilon_o/\mu_o)^{1/2}$ is the wave admittance of free space. In formulating these relations, reflection losses at the interfaces have been ignored so that $P_o \approx P_i$ holds. This is in accord with the experimental technique [6] where the efficiency η_B of the Bragg reflection in the core region is measured as the ratio of the powers of the external Bragg-reflected (P_B) beam and the transmitted (P_T) beam.

$$\eta_B \;=\; P_B/P_o \;\approx\; P_B/P_T \tag{13}$$

These beams suffer identical reflection losses at each interface because their directions of propagation and polarization are symmetrically equivalent. Therefore, their ratio remains unchanged at each refraction. Moreover, because $\eta_B \ll 1$, the value of η_B is essentially the same regardless of whether it is referred to the power of the incident or of the transmitted beam.

In summary then, the excitation of the grating by the probe beam is described by the distribution of dipole moments

$$d\mathbf{q} \;=\; 2\, n_o \,\epsilon_o \, h(x,y)\, \Delta n(z)\, \cos(Kz)\, \mathbf{E}_o(x,y,z)\, dx\, dy\, dz \tag{14}$$

III. Radiation of the fiber grating

A. Output field

The field amplitude and power density radiated from the grating to some distant point $\mathbf{R}$ are obtained by summing the radiations of all contributing dipoles $d\mathbf{q}$. All three dimensions of the source region are large compared to the wavelength. Therefore, constructive interference can occur only when input and output directions are within narrow angular ranges. In all other situations the contributions from the dipoles $d\mathbf{q}$ interfere destructively.

For a quantitative formulation we start by considering an elementary dipole $d\mathbf{q}$ located at the origin of a space filled homogeneously with index n_o. The direction of $d\mathbf{q}$ is parallel to the polarization $\mathbf{E}_o$ of the probe beam. At a general point $\mathbf{R}$ in space the electromagnetic field emitted by the dipole $d\mathbf{q}$ is characterized [9] by a vector potential $d\mathbf{A}$ which is retarded by $\mathbf{kR}$.

$$d\mathbf{A}(\mathbf{R}) \;=\; \frac{j\,\mu_o\,\omega}{4\,\pi R}\; e^{-j\mathbf{kR}}\; d\mathbf{q} \tag{15}$$

Here $R = |\mathbf{R}|$ is the distance from the origin, and $\mathbf{k} = n_o\,k\,\mathbf{R}/R$ is the propagation vector in the direction to $\mathbf{R}$. The contribution of $d\mathbf{q}$ to the electric field in the outgoing beam is obtained as the time derivative, $d\mathbf{E} = -j\omega\,d\mathbf{A}$ from $d\mathbf{A}$. In the far field only that component $d\mathbf{E}_B$ remains which is normal to $\mathbf{R}$. It results, in turn, from the normal component $d\mathbf{q}_\perp$, where the subscript $\perp$ indicates the component of $d\mathbf{q}$ normal to $d\mathbf{R}$. Applying this relation now to each dipole $d\mathbf{q}(\mathbf{r})$ in the excited region of the grating, the retardation must be corrected by $\mathbf{kr}$ to account for that location$\mathbf{r}$, and using (5) and (6), integration over the entire source region where $G(\mathbf{r}) \neq 0$ yields the far field of the scattered radiation.

$$\mathbf{E}_B(\mathbf{R}) \;=\; \frac{\mu_o\,\omega^2}{4\,\pi R} \int \delta\epsilon(\mathbf{r})\,\mathbf{E}_{o\perp}(\mathbf{r})\,e^{-j\mathbf{k}(\mathbf{R}-\mathbf{r})}\;dV \tag{16}$$

$$\;=\; \frac{k^2\,n_o}{4\,\pi R}\;\hat{\mathbf{E}}_{o\perp} \int \delta n(\mathbf{r})\,G(\mathbf{r})\;\left[e^{+j\mathbf{Kr}} + e^{-j\mathbf{Kr}}\right]\;e^{j(\mathbf{k}-\mathbf{k}_o)\mathbf{r}-jn_okR}\;dV \tag{17}$$

In the last line we have introduced a grating vector $\mathbf{K}$ normal to the index planes of the fiber grating, with $|\mathbf{K}| = K = 2\pi/g$. As we treat here only the case of a grating with non-slanted index planes, $\mathbf{K} = \{0, 0, K\}$, and we have $\mathbf{Kr} = Kz$.

B. Bragg reflected beam

In a typical experimental situation this field is a narrow beam. We recognize this fact by noting that a strong field $\mathbf{E}_B(\mathbf{R})$ can result only at points $\mathbf{R}$ where the phase of the integrand is stationary. Closer inspection reveals that only the term $\exp(+j\mathbf{Kr})$ in the bracket in (17) contributes significantly to the integral, representing the +1st diffraction order. The other term, representing the -1st order, has a rapidly varying phase and does, therefore, not produce a significant output in the far field. For the +1st order, then, stationarity of the phase ('phase match') requires that the following vector sum should vanish

$$\mathbf{k} \;-\; \mathbf{k}_o \;+\; \mathbf{K} \;\longrightarrow\; 0 \tag{18}$$

When combined with the conditions $|\mathbf{k}_o| = |\mathbf{k}| = n_ok$ which must hold for the input and output beams, this requirement Eq.(18) represents the Bragg condition Eq.(4) formulated earlier, including the symmetry $\psi_o = \theta_o$.

The particular output vector $\mathbf{k}$ which satisfies Eq.(18) is characteristic of the Bragg situation. It will be denoted in the following by $\mathbf{k}_B = n_ok\{-\cos\psi_o,\, 0,\, -\sin\psi_o\}$. Likewise the input vector which satisfies the Bragg condition is $\mathbf{k}_o = n_ok\{-\cos\theta_o,\, 0,\, +\sin\theta_o\}$. Accordingly the Bragg output direction k_B is obtained by 'reflecting' the Bragg input direction k_o at the index planes of the grating, which means $\psi_o = \theta_o$, see Fig. 2. This symmetry had been expressed earlier in Eq.(4).

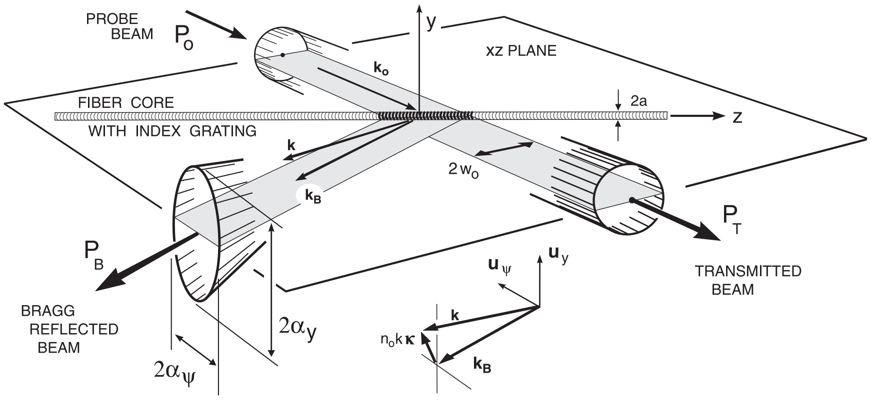

Fig. 2

Figure 2: Bragg diffraction of a probe beam of circular cross-section with $w_o \gg a$. The angular width α_y of the diffracted beam normal to the xz plane is wider than the width α_ψ in that plane.

In the following we continue to consider this Bragg situation with an input beam along $\mathbf{k}_o$, and we analyze in more detail the angular distribution of radiation in output directions close to $\mathbf{k}_B$. We distinguish these directions by introducing a dimensionless vector $\boldsymbol{\kappa}$ which specifies the angular deviation of the actual direction of observation from the Bragg direction $\mathbf{k}_B$.

$$\mathbf{k} \;=\; \mathbf{k}_B \;+\; n_o\, k\, \boldsymbol{\kappa} \tag{19}$$

The condition $|\mathbf{k}| \;=\; |\mathbf{k}_o| \;=\; n_o k$ is satisfied if $\boldsymbol{\kappa}$ is orthogonal to $\mathbf{k}_B$ and small, $(\boldsymbol{\kappa}\,\mathbf{k}_B) = 0$ and $|\boldsymbol{\kappa}| \ll 1$. For a practical interpretation, $\boldsymbol{\kappa}$ is split up into its orthogonal components

$$\boldsymbol{\kappa} \;=\; \kappa_y\, \mathbf{u}_y \;+\; \kappa_\psi\, \mathbf{u}_\psi \tag{20}$$

where $\mathbf{u}_y = \{0, 1, 0\}$ is the unit vector normal to the xz plane and $\mathbf{u}_\psi = \{\sin\theta_o,\, 0, -\cos\theta_o\}$ a unit vector in that plane, so that $\mathbf{k}_B,\;\mathbf{u}_y$, and $\;\mathbf{u}_\psi$ form a right-handed coordinate system, see Fig. 2. Obviously, then, κ_ψ is the angular deviation of the observation direction $\mathbf{k}$ from the Bragg direction $\mathbf{k}_B$, measured in the projection on the xz plane. Correspondingly, κ_y is the tilt angle of $\mathbf{k}$ out of the xz plane, i.e. the angular deviation along the y direction.

Using this vector $\boldsymbol{\kappa}$ and the separation (6), the field amplitude in the outgoing beam is

$$\mathbf{E}_B(\mathbf{R}) \quad = \quad -\,\frac{n_o}{4\,k\,R}\,\Delta n\; g(\boldsymbol{\kappa})\;\hat{\mathbf{E}}_{o\perp}\, e^{-j\mathbf{k}\mathbf{R}} \tag{21}$$

where
$$g(\boldsymbol{\kappa}) \quad = \quad k^3 \int_{(core)} h(x,y)\, G(x,y,z)\, e^{j\, n_o\, k\, \boldsymbol{\kappa}\mathbf{r}}\, dV \tag{22}$$

In going from Eq.(17) to (21) it has been assumed that $\Delta n(z)$ is varying so slowly that it may be considered as constant along the width $2w_z$ of the probe beam. The dimensionless function $g(\boldsymbol{\kappa})$ describes the angular spread of the output field about the direction $\mathbf{k}_B$. As might have been expected in the weak scattering approximation, this distribution $g(\boldsymbol{\kappa})$ is the Fourier transform of the amplitude distribution $G(\mathbf{r})$ in the source region, weighted by the transverse index profile $h(x,y)$ of the grating.

From Eq.(21) the power density $p_B(\mathbf{R})$ in the Bragg-reflected beam is found as $p_B(\mathbf{R}) = (1/2) n_o Y_o |\mathbf{E}_B|^2$. A related quantity, independent of the distance R, is the radiance of the output beam, $\mathcal{R}_B(\boldsymbol{\kappa}) \equiv dP_B/d\Omega = R^2 p_B(\mathbf{R})$. Here $d\Omega$ denotes the element of solid angle. In calculating $\mathcal{R}_B(\boldsymbol{\kappa})$ we express the peak amplitude $\hat{\mathbf{E}}_o$ of the probe beam by the peak power density $\hat{p}_o$ using Eq.(12). We also introduce here the angle γ_o, which is included between the direction $\mathbf{E}_o$ of the input polarization and $\mathbf{k}_B$, the Bragg output direction. Using this angle $|\hat{\mathbf{E}}_{o\perp}|^2 = |\hat{\mathbf{E}}_o|^2 \sin^2\gamma_o$. When the input polarization is directed along the y axis and the output direction $\mathbf{R}$ is close to the xz plane (s-polarization) we have $\gamma_o \approx \pi/2$ and $\sin^2\gamma_o \approx 1$. We obtain the angular distribution of radiance,

$$\mathcal{R}_B(\boldsymbol{\kappa}) \;=\; \frac{n_o^2}{8\,\pi^3\,k^2}\,\Delta n^2\,\hat{p}_o\,|g(\boldsymbol{\kappa})|^2\,\sin^2\gamma_o. \tag{23}$$

Integration of this expression over all directions $\boldsymbol{\kappa}$ yields the total Bragg reflected power, $P_B = \int \mathcal{R}_B(\boldsymbol{\kappa}) d\Omega$. Two other quantities convenient for comparison with the experiment are the diffraction efficiency $\eta_B = P_B/P_o$, and the total scattering cross-section σ_B, defined here by the relation $P_B = \sigma_B\,\hat{p}_o$.

$$\sigma_B \;=\; \frac{\pi}{2}\,w_o^2\,\eta_B \;=\; \frac{n_o^2}{8\,\pi^3\,k^2}\,\Delta n^2\,g_o^2\,\Delta\Omega_B\,\sin^2\gamma_o \tag{24}$$

where $$g_o \;\equiv\; g(\boldsymbol{\kappa}=0) \;\approx\; \pi^{3/2}\,k^3\,a^2\,w_o\,/\cos\psi_o \tag{25}$$

and $$\Delta\Omega_B \;=\; g_o^{-2}\int |g(\boldsymbol{\kappa})|^2\,d\Omega \;=\; \Delta\kappa_\psi\,\Delta\kappa_y \tag{26}$$

The quantity $\Delta\Omega_B$ introduced here has the meaning of an average solid angle of the output beam in the sense that the total power in the output beam may be written as $P_B = \hat{\mathcal{R}}_B\,\Delta\Omega_B$, where $\hat{\mathcal{R}}_B$ is the radiance on the beam axis ($\boldsymbol{\kappa}$=0). In the same sense, the average full angular apertures $\Delta\kappa_\psi$ and $\Delta\kappa_y$ along the directions κ_ψ and κ_y, respectively, have been introduced in Eq.(26).

Anticipating for these angular apertures the results which will be derived only below, we can complete here the derivation of the total Bragg reflected power, expressed by the scattering cross-section σ_B or by the diffraction efficiency η_B. For a non-slanted fiber grating which is homogeneous across the core $[h(x,y) = 1]$ and which is probed at the Bragg input angle θ_o by a Gaussian beam of waist radius $w_o \gg a$ we have

$$\Delta\kappa_\psi \;=\; \sqrt{2\pi}/(n_o\,k\,w_o) \tag{27}$$

$$\Delta\kappa_y \;=\; 2 f_I/(n_o\,k\,a) \tag{28}$$

$$\sigma_B(z_o) \;=\; 0.5\,\pi^{1/2} f_I\,k^2\,a^3\,w_o\,\Delta n^2(z_o)\,\sin^2\gamma_o\,/\cos^2\theta_o \tag{29}$$

$$\eta_B(z_o) \;=\; \pi^{-1/2} f_I\,k^2\,(a^3/w_o)\,\Delta n^2(z_o)\,\sin^2\gamma_o\,/\cos^2\theta_o \tag{30}$$

The numerical factor f_I used in these equations is $f_I = \int_0^\infty 4x^{-2} J_1(x) dx \approx 1.69$, resulting from integration of Eq.(26) The argument z_o, which denotes the beam position along the fiber, has been re-introduced here in order to indicate the purpose of these relations in analyzing the axial distribution of the modulation amplitude $\Delta n(z_o)$.

Employing these results, the initial experiments reported in Ref. [6] on the determination of $\Delta n(z)$ from the measured diffraction efficiency have shown satisfactory agreement with the envelope expected from the writing conditions. This hold true despite the regrettable fact that the numerical factor $0.5 f_I \sqrt{\pi} \approx 1.50$ in front of Eq.(29) has been given erroneously as 1.66 in Ref. [6]

C. Angular characteristics of Bragg reflex

The angular distribution of the radiance $\mathcal{R}(\boldsymbol{\kappa})$ in the outgoing beam is governed by the function $|g(\boldsymbol{\kappa})|^2$. The defining equation Eq.(22) is a Fourier integral which can be evaluated in closed form if the grating is homogeneous across the core, $h(x,y) = 1$, and if the probe beam is much wider than the core ($w_o \gg a$), as had been postulated. In this limit, the excitation $G(\mathbf{r})$ may be assumed to be constant within any cross-section z of the fiber core. Expressing explicitly the dependence on both angular components of $\boldsymbol{\kappa}$,

$$|g(\kappa_\psi,\, \kappa_y)|^2 = g_o^2\ \Gamma^2(\bar{\kappa}/\alpha_y)\ e^{-2\kappa_\psi^2/\alpha_\psi^2} \tag{31}$$

where

$$\Gamma(\xi) = J_1(2\xi)/\xi \tag{32}$$

$$\bar{\kappa} = (\kappa_y^2 + \kappa_\psi^2 \sin^2\theta_o)^{1/2} \tag{33}$$

$$\alpha_y = 2/(n_o\, k\, a) \tag{34}$$

$$\alpha_\psi = 2/(n_o\, k\, w_o) \tag{35}$$

The angular spread of the Bragg reflected beam in the xz plane is dominated by the Gaussian distribution $e^{-2\kappa_\psi^2/\alpha_\psi^2}$. This term can be shown to be identical to the angular spread of the incident probe beam, assuming again $w_o \gg a$. Correspondingly, the angular distributions of input and output beams in the xz plane agree. They are characterized by the same e^{-2} angular power widths, $\alpha_\theta = \alpha_\psi$, see Fig. 2.

Along the orthogonal direction κ_y the angular spread of the Bragg reflected beam is described by the function $\Gamma^2(\xi)$, which is plotted in Fig. 3. For most of the angular beam profile, where $|\kappa_y| \gg |\kappa_\psi| \sin\theta_o$, the argument $(\bar{\kappa}/a_y)$ of Γ^2 is essentially identical to the ratio (κ_y/a_y). For that part of the beam, the influence of the term $|\kappa_\psi|$ in Γ^2 is negligible and, therefore, the Gaussian $e^{-2\kappa_\psi^2/\alpha_\psi^2}$ does indeed describe there the full dependence on κ_ψ. In that part, the profile function $|g(\kappa_\psi,\, \kappa_y)|^2$ can be separated into a ψ-dependent and a y-dependent part. The beam width along the y direction is characterized by α_y, with the e^{-2} power points at $\kappa_y \approx 1.3\,\alpha_y$. Because we had postulated that the probe beam is much wider than the fiber core, it follows from Eq.(28) that the angular aperture of the Bragg reflected beam is much wider along the y direction than along ψ, with $\alpha_y/\alpha_\psi = w_o/a \gg 1$. This situation was depicted in Fig. 2. Moreover, because the core radius is large compared to the wavelength, $a \gg \lambda$, both angular apertures are small, $\alpha_\psi \ll \alpha_y \ll 1$, and the output field has indeed the form of a narrow beam.

For directions extremely close to the xz plane and in the wings of the ψ distribution, where $|\kappa_y| < |\kappa_\psi| \sin\psi_o$, however, the angular distribution cannot be factorized in unconnected ψ and y dependencies, because κ_ψ dominates $\bar{\kappa}$. In reality this is irrelevant, because for these directions near the beam axis, $|\kappa_y| < \alpha_\psi$, and the bracket is ≈ 1, whereas for larger angles, $|\kappa_y| > \alpha_\psi$, the exponential term in Eq.(31) vanishes rapidly. In this sense, the distribution $|g(\kappa_\psi,\, \kappa_y)|^2$ can well be factorized in the entire $\boldsymbol{\kappa}$ range where it has significant power. Using this fact, the mean angular widths $\Delta\kappa_\psi$ and $\Delta\kappa_y$ of the Bragg

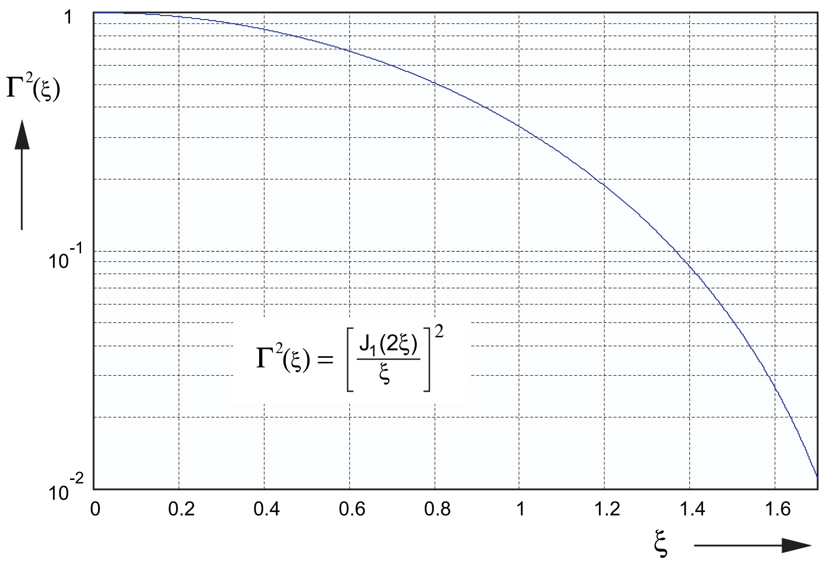

Fig. 3

Figure 3: The function $\Gamma^2(\xi) = [J_1(2\xi)/\xi]^2$ shows the angular distribution of power along the direction $\bar{\kappa}_y$. Simultaneously, this function describes the reduction of the Bragg diffracted power when the input angle deviates from the Bragg direction by $\delta\theta_i = \xi/[n_o ka \tan\theta_o/\tan\theta_i]$.

reflected beam have been evaluated, which had already been used earlier in Eq.(26) - (28) to calculate the total power of the Bragg reflected beam.

$$\Delta\kappa_\psi \equiv g_o^{-2} \int g^2(\kappa_\psi, 0)\, d\kappa_\psi = \sqrt{\pi/2}\, \alpha_\psi \tag{36}$$

$$\Delta\kappa_y \equiv g_o^{-2} \int g^2(0, \kappa_y)\, d\kappa_y \approx 1.19\, \alpha_y \tag{37}$$

A reminder may be appropriate at this point that all angular widths discussed here refer to the core medium of index n_o. The angles outside the fiber are related by refraction, see Eq.(3).

IV. Discussion

A. Measurement of index modulation $\Delta n(z)$

It had been the primary goal of this paper to establish the relationship between the envelope function $\Delta n(z)$ of the index modulation and the reflection efficiency of a fiber grating. This problem is solved for the homogeneous non-slanted grating by Eq.(30). This equation permits evaluation of $\Delta n(z)$ from the measured diffraction efficiency η_B. That equation may also be used to optimize the experimental conditions to give an output beam of maximum power and spatial resolution, and we can estimate from it the smallest observable Δn.

(a) Output power and spatial resolution.
An obvious first strategy in maximizing the Bragg reflected power is to use a probe beam which is polarized normal to the plane of incidence (**s** polarization). For this field direction the factor $\sin^2\gamma_o$ in Eq.(30) assumes its maximum. A second, more significant parameter in Eq.(30) is the beam radius w_o which can be chosen freely by the design of the focusing optics of the probe beam. The choice of w_o determines the attainable spatial resolution, because

the index profile $\Delta n(z)$ is averaged over a distance of $\approx 2w_z = 2w_o/\cos\theta_o$. Moreover w_o affects the output power P_B, because it appears in the denominator of Eq.(30). It is a fortunate situation that both the resolution and the power improve simultaneously when the beam radius is reduced. Therefore the smallest possible beam width w_o should be used which is compatible with the condition $w_o \gg a$ which limits the applicability of Eq.(30). Although that limit has not been analyzed in detail, it is estimated that meaningful values of Δn are obtained as long as $w/a \geq 1.5 \ldots 2$. Experimentally [6] this means an optimum beam diameter of $2w_i \approx 10\,\mu$m. This value is also the spatial resolution in the determination of Δn.

(b) Measurement of small Δn

The limit down to which an index modulation Δn can be measured is given by the smallest Bragg diffracted power discernible from noise and other radiation. Using the mentioned narrow beam width, the diffraction efficiency is of the order of magnitude $\eta_B \sim k^2 a^2 \Delta n^2$. For a grating in a typical single-mode $1.5\,\mu$m communication fiber, measured at $\lambda = 0.633\,\mu$m, this efficiency is $\eta_B \sim 10^3 \Delta n^2$. With that estimate we can predict for a strong fiber grating ($\Delta n = 10^{-3}$) an efficiency of $\eta_B \approx 10^{-3}$, as observed experimentally. [6] On the other hand, the smallest diffraction efficiency measurable with lock-in techniques and a probe beam of a few milliwatts is estimated to be of the order $\eta_{B,min} \sim 10^{-9}$. Accordingly the minimum detectable index modulation is $\Delta n_{min} \sim 10^{-6}$, also in reasonable agreement with experimental observation. [10]

(c) Inhomogeneous gratings

When the Ge concentration in the fiber core is so high that there is significant attenuation of the UV writing light across the core, inhomogeneous gratings result. They were excluded from the derivation given here. Nevertheless, the discussion shows that characteristic information on such gratings can be obtained from the angular distribution of the radiance $\mathcal{R}_B(\boldsymbol{\kappa})$ in their output beam. In particular, the radiance $\hat{\mathcal{R}}_B = \mathcal{R}_B(0)$ on the beam axis ($\boldsymbol{\kappa} = 0$) is proportional to g_o^2 according to Eq.(23). Apart from constant factors, g_o represents the average or integral index modulation,

$$g_o \quad \propto \quad \overline{\Delta n} \quad \propto \quad \int_{core} h(x,y)\;\Delta n(z)\;G(x,y,z)\;dV \quad \propto \quad \Delta n \int_{core} h(x,y)\;dx\,dy \tag{38}$$

These proportionalities derive from Eq.(22) for $\boldsymbol{\kappa} = 0$ in the limit $w_o \gg a$. Therefore, it should be possible to determine the average index modulation $\overline{\Delta n}$ of an inhomogeneous grating by measuring the radiance on the axis of its Bragg reflex. The inhomogeneity only affects the off-axis radiance. A homogeneous and an inhomogeneous grating with the same $\overline{\Delta n}$ produce equal radiances $\mathcal{R}_B(0)$ on the axis when measured with a given probe beam. However, depending on the azimuthal orientation of the grating, the inhomogeneous grating will generally have a wider radiation lobe ($\Delta\alpha_y$ and $\Delta\kappa_y$) and, therefore, a higher diffraction efficiency than the homogeneous grating. As a consequence, evaluation of the index modulation from Eq.(30) tends to overestimate Δn when the grating is inhomogeneous.

B. Tolerances of adjustments

As the diffraction efficiency η_B had been derived only for the perfect Bragg situation, it is of interest to find the tolerances which are permissible in the adjustment of that situation.

(a) Angle of incidence.

A first critical parameter is the angle of incidence, θ_i, which determines the angle θ_o in

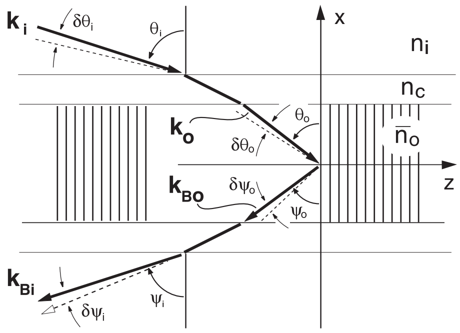

Figure 4: A deviation $\delta\theta_i$ of the input direction (dashed) from the Bragg direction θ_i (full line) results in a deviation $\delta\psi_i = -\delta\theta_i$ of the output direction. This situation is typical of a 'thin' grating.

the core region. A small misalignment $\delta\theta_i$ of this angle (see Fig. 4) has two effects on the output beam, a change in direction and a reduction of power. To quantify these effects we introduce formally a modification $\boldsymbol{\kappa}_o$ to the input vector $\mathbf{k_o}$, in close analogy to $\boldsymbol{\kappa}$ which had been defined in Eq.(19) for the output direction $\mathbf{k}$. This modification leads to an extra term $-jn_o k\boldsymbol{\kappa}_o\mathbf{r}$ in the exponents of Eqs.(17) and (22), and an extra vector $-jn_o k\boldsymbol{\kappa}_o$ in the phase matching condition Eq.(18). With $w_o \gg a$, only the z component of that condition is relevant for the direction of the output beam. Its axis shifts from $\boldsymbol{\kappa} = 0$ to a new angular orientation in the xz plane characterized by $\kappa_z = \kappa_{o,z}$, where the subscript z indicates the z component. When expressed in variations of the angles, this condition is equivalent to $\delta\psi_i = -\delta\theta_i = -(\tan\theta_i/\tan\theta_o)\,\delta\theta_o$ in the notation of Fig. 4. When the input beam is rotated about the y axis by a small amount $\delta\theta_i$ off the Bragg condition, the output beam swings *in the same sense* about the y axis, so that the angle $(\theta_i + \psi_i)$ included between the input and output directions remains fixed. This is contrary to the behavior of a hypothetical mirror (xy plane) which would exhibit a Bragg 'reflection' of the incident beam. Closer investigation shows that such a 'reflection' would exist in the limit $w_o \ll a$. In the present situation, however, the behavior is characteristic of a 'thin' diffraction grating ($a \ll w_o$).

The reduction of the output power associated with a deviation $\delta\theta_i$ is found from Eq.(22). When the z component of the phase matching condition Eq.(18) is satisfied and determines the output direction ψ_o, a mismatch $2\kappa_x$ remains in the x component, because the vectors $\boldsymbol{\kappa}$ and $\boldsymbol{\kappa}_o$ are bound to be orthogonal to $\mathbf{k}$ and $\mathbf{k}_o$, respectively. With $\kappa_x \approx \cos\theta_o\ \delta\psi_o$ the Fourier integral Eq.(22) yields for a homogeneous grating a reduction of the power by the factor $\Gamma^2(\xi)$ with the same function Γ which had been defined in Eq.(32), but used here with the argument $\xi = n_o ka(\tan\theta_o/\tan\theta_i)\delta\theta_i$. It follows from Fig. 3 that the power is reduced by 3 dB when the argument of Γ reaches $\xi \approx 0.81$. For a typical situation [6] this corresponds to a misalignment angle of $\delta\theta_i \approx 1\,\mathrm{deg}$. This result indicates how critical a correct adjustment of the input angle θ_i is. It should be set to within $\pm\,0.1\,\mathrm{deg}$ of the Bragg condition, characterized by the maximum of the output power P_B.

(b) Adjustment of focus

It may appear that the position of the focus of the probe beam is a second critical parameter because it must be adjusted to coincide with the fiber axis, see Figs. 1(c,d). The tolerance of that adjustment transverse to the beam is simply a small fraction of the waist radius w_i. Focussing along the input beam should be correct to a fraction of the beam parameter $b_o = 2\pi w_o^2 n_o/\lambda$ of the probe beam in the core region. In the limit $w_o \gg a$, the beam is fairly well collimated, and the beam parameter is conveniently large, typically $b_o > 0.3\,\mathrm{mm}$. Therefore, the problem in adjusting the focus is mainly one of finding a convenient criterion for the correct focal position. Systematic variation of the focus and careful observation of the resulting structure of the transmitted beam permit identification of the correct focal position.

C. Measurement of the grating period $g(z)$

The basic diffraction arrangement [Fig. 1(a)] permits a direct determination of the grating period, g, from the angle of diffraction. The period thus determined is an average over the width $2w_o$ of the probe beam. By scanning the beam position z_o along the grating, its chirp function $g(z)$ can be obtained, too.

(a) Uniform grating
The grating period may be found either from the Bragg angle θ_o which gives maximum diffraction efficiency, or from the angle $(\theta_i + \psi_i)$ of angular deflection by the grating. It will be shown now that it is highly preferable to determine g from the deflection angle rather than from the Bragg angle.

The period determined this way from Eq.(1) is $g = \lambda/[2n_i(\sin\theta_i + \sin\psi)]$. This value is insensitive to small misalignments $\delta\theta_i$ of the input direction, because the earlier discussion of the relationship between input and output directions had revealed that for small misalignments $\delta\theta_i + \delta\psi_i = \delta(\theta_i + \psi_i) = 0$. As mentioned above, this value of g is independent of the core index n_o of the fiber and, in particular, of any change of the mean core index due to the UV exposure. However, the quantity which is actually of interest in Bragg applications, is the central wavelength $\lambda_B = 2\overline{n_o}g$ of guided Bragg reflection, and this quantity does depend on $\overline{n_o}$ and on the mentioned index change. Therefore, an independent method is required for the determination of $\overline{n_o}$.

To achieve a high accuracy in the determination of g the directions of incident and transmitted beam should be sharply defined in the θ and ψ dimensions, respectively. According to Eq.(35) a large beam width w_o must be used. This demand runs contrary to the condition appropriate in the measurement of Δn, where a narrow beam is preferable for a high diffraction efficiency. The reduction of η_B resulting from a large w_o may be compensated, however, by the use of an astigmatic input beam, focused by a cylindrical optical system to a broad width w_o *in* the xz plane and a narrow width w_y normal to that plane. This scheme would bring up the efficiency by a factor w_o/w_y. Experimentally, using a high quality focusing lens, beam widths of up to $w_o \geq 1000\,a \approx 4\,\mathrm{mm}$ can readily be employed. The resulting angular width is $\alpha_\psi \lesssim 3\cdot 10^{-5}$. With a precision goniometer, then, the beam deflection may be measured to an angular accuracy of 10^{-5} radiant or better. Correspondingly the accuracy in determining the grating period can reach $\delta g/g \approx 10^{-5}$ or better. The wavelength λ and the index n_i must be known to a corresponding precision.

(b) Chirped grating
In weakly chirped gratings, as used for the dispersion compensation of optical fiber links [2], the period length may be characterized by the first terms of a series expansion,

$$g(z) \;=\; g(z_o)\,[1 \;+\; (z - z_o)\,C(z_o)\;\ldots] \tag{39}$$

where z_o denotes the position of the beam axis and $C(z_o)$ is the local chirp rate. With such a grating the angular width α_ψ of the Bragg reflex is given by Eq.(35) only if the period $g(z)$ is sufficiently constant within the width $2w_o$ of the probed region of the grating. The limit up to which this condition holds is reached when the width α_ψ equals the angular spread of the output beam, $2\delta\psi_o = -2\tan\theta_o \delta g/g$, resulting from the chirp. This relation follows from Eq.(7) for a variation δg, taking into account that the input direction is fixed and, therefore, the output direction changes by $2\delta\theta_o$. We identify δg with the variation of $g(z)$ along the beam radius, $\delta g = Cgw_o$, and obtain a condition for the maximum beam radius up to which the chirp causes negligible broadening of the diffracted beam.

$$w_{o,max}^2 = [\, n_o \, k \, C \, \tan\theta_o \,]^{-1} \tag{40}$$

As a practical example we consider a fiber grating for the compensation of $20\,\mathrm{ps}^2/\mathrm{km}$ dispersion along a 100 km fiber. [2]. This grating must be $\approx 4\,\mathrm{cm}$ long and have a chirp rate of $C = 4 \cdot 10^{-6}/\mathrm{mm}$. With these data Eq.(40) yield a maximum beam radius of $w_{o,max} \approx 4\,\mathrm{mm}$. At such a width, as mentioned, the local period may be determined with a relative accuracy of $\delta g/g \approx 5 \cdot 10^{-5}$. It remains to be seen how this method will perform in reality.

References

[1] K. O. Hill, B. Malo, F. Bilodea; and D. C. Johnson, "Photosensitivity in optical fibers", Annual Review of Material Science, Vol. 23, pp 125 - 157, 1993.

[2] F. Ouellette, J.-F. Cliche, and S. Gagnon, "All-fiber devices for chromatic dispersion compensation based on chirped distributed resonant coupling", J. Lightwave Technol., vol.12, pp.1728 - 1738, Oct. 1994.

[3] K. P. Koo and A. D. Kersey, "Bragg grating-based Laser Sensors System with Interferometric Interrogation and Wavelength Multiplexing", J. Lightwave Technol., vol.13, pp.1243 - 1249, July 1995.

[4] J. A. R. Williams, I. Bennion, and N. J. Doran, "The design of in-fiber Bragg grating systems for cubic and quadratic dispersion compensation", Optics Communications, vol 116, pp. 62 - 66 (1995).

[5] E. Brinkmeyer, "Simple algorithm for reconstructing fiber gratings from reflectometric data", Opt. Lett. vol. 20, pp. 810-812, April 1995.

[6] P.A. Krug, R. Stolte, and R. Ulrich, "Measurement of index modulation along an optical fibre Bragg grating", Opt. Lett., vol.20, No. 17, pp.1767-1769, Sept. 1995.

[7] E. Hecht and A. Zajac, "Optics", Addison-Wesley Publishing Co., Reading, Mass, USA, 1974.

[8] R. J. Campbell and R. Kashyap, "The properties and applications of photosensitive germanosilicate fibre", Int. J. Optoelectron. vol. 9, pp. 33 - 57, (1994).

[9] S. Ramo, J. R. Whinnery, and T. van Duzer, "Fields and waves in communication electronics", Wiley & Sons, New York NY, 1967.

[10] F. Ouellette, P.A. Krug, and R. Pasman, "Characterization of long phase masks for writing fibre Bragg gratings", Conf. on Photosensitivity and Quadratic Nonlinearities in Glass Waveguides, Portland, Oregon, USA, 9-11 Sept. 1995.